ELSEVIER

Journal of Molecular Catalysis A: Chemical 100 (1995) 103–114

JOURNAL OF MOLECULAR CATALYSIS A: CHEMICAL

Defect processes at low coordinate surface sites of MgO and their role in the partial oxidation of hydrocarbons

Dewi W. Lewis [a], Robin W. Grimes [b], C. Richard A. Catlow [a,*]

[a] *Davy Faraday Research Laboratory, The Royal Institution of Great Britain, 21 Albemarle St., London W1X 4BS, UK*

[b] *Department of Materials, Imperial College, Prince Consort Rd., London SW7 2BP, UK*

Abstract

Atomistic simulation techniques have been used to study the bulk and surface defect chemistry of MgO and Li/MgO catalysts. The energetics and stability of defects, particularly those which are thought to influence the activity of the catalysts, have been investigated. Of particular note is the enhanced stability of hole and substitutional defects at low-coordinate sites, both at steps and small protosteps. From the results of our calculations we comment generally on the factors controlling the overall activity of these catalysts.

Keywords: MgO; Defect structures; Oxidation catalysis; Computer simulation

1. Introduction

Defects in solids play a crucial role in controlling the activity of heterogeneous solid catalysts. Indeed, it is the defect chemistry which often controls the structure of active sites. Moreover, since catalysis is a surface process, it is of critical importance that we understand the differences between the surface defect chemistry and that of the bulk. In this paper, atomistic simulation techniques are employed to study the defects present in MgO and Li/MgO catalysts, with particular attention to their potential role in the use of these materials as partial oxidation catalysts.

Li/MgO is found to produce reasonable yields of ethane and ethene when methane is passed over the material at ca. 700°C [1–7]. Oxygen is also required in the reaction stream and it is further noted that pure MgO has only a limited activity [8,9]. The primary active site for this reaction is believed to be an oxygen hole species [3–6] which initiates the reaction by abstracting a hydrogen from a methane molecule:

$$CH_4 + O^-_{(s)} \rightarrow CH^{\cdot}_{3(g)} + (OH)^-_{(s)} \quad (1)$$

This surface hole species can either be an intrinsic defect or, most likely, is formed as a consequence of the presence of lithium. Moreover, lithium stabilises the hole species through the formation of the neutral lithium trapped hole, $[Li^+O^-]$; denoted as $[Li]^O$ throughout this paper. Ethane is produced by gas phase combination of the methyl radicals:

$$CH^{\cdot}_{3(g)} \rightarrow C_2H_{6(g)} \quad (2)$$

Undesirable products such as CO and CO_2 are also formed in the gas phase by recombination of the methyl radicals with gas phase oxygen. However,

* Corresponding author.

SSDI 1381-1169(95)00160-3

C_2 products are favoured at high temperatures; kinetic factors are therefore clearly important. Ethene is formed by the dehydrogenation of ethane and not via methylene carbene [10] and therefore sites other than $[Li]^O$ may be present for ethane dehydrogenation. The active site is regenerated by the formation of water and the absorption of gas phase oxygen:

$$2OH^-_{(s)} \rightarrow O^{2-}_{(s)} + V^{\cdot\cdot}_O + H_2O_{(g)} \quad (3)$$

$$O^{2-}_{(s)} + V^{\cdot\cdot}_O + \tfrac{1}{2}O_{2(g)} \rightarrow 2O^-_{(s)} \quad (4)$$

where $V^{\cdot\cdot}_O$ is a vacant surface oxygen site.

Although there is a general consensus regarding the nature of the active site for methane activation in Li/MgO, the nature of the active site in pure MgO and active sites for the formation of other products are less well characterised. Recent work has demonstrated the importance of the morphology [9] and the bottom of surface steps have been suggested as active sites for methane activation in the undoped MgO. Such low coordinate sites have previously been considered as possible active sites, particularly in theoretical studies [11–14]. However, there is no direct experimental measurement of reactions at such sites.

The binary metal oxides have long been investigated using the lattice simulation techniques employed here [15]. The nature of the work has mirrored the experimental interest in the materials. Earlier work concentrated on the modelling of the crystal structure and of intrinsic defects in MgO and related materials [16] and in defects caused by radiation damage [17]. Following the work of Ito and Lunsford [2] theoretical studies were performed on likely active sites on planar [13,18–20] and non-planar surfaces [21].

The present paper will build on these earlier theoretical studies in order to amplify our understanding of the surface chemistry of pure and Li doped MgO. A key feature of our results is the demonstration of the role of low coordinate sites as trapping sites for dopant/hole centres which as noted are almost certainly the major active sites in these materials.

2. Methodology

We have used standard lattice energy minimisation techniques using effective interatomic potentials. We present only a brief outline; more extensive descriptions are given elsewhere [22]. The method is based on the Born model of the ionic solid. The total lattice energy of a system can be expressed as:

$$U_{\text{latt}} = \frac{1}{2}\sum_{i=1}^{N}\sum_{j=1,j\neq i}\frac{q_iq_j}{r_{ij}} + \frac{1}{2}\sum_{i=1}^{N}\sum_{j=1,j\neq i}\left(A\exp\left(\frac{-r_{ij}}{\rho}\right) - \frac{C}{r_{ij}^6}\right) \quad (5)$$

where the first term is the sum of the Coulombic interactions and the second term, in the form of a Buckingham potential, describes the short range interactions. The summation over i extends to all N ions in the unit cell and the summation over j extends over all ions to infinity in the case of the Coulombic term, and over all ions within a cut-off distance of ion i for the short range interactions. Ionic polarisability is included using the shell model [23], where a massless shell, representing the polarisable valence electrons is connected to a core (with mass) by an harmonic spring. The polarisability of a free ion can then be expressed as

$$\alpha = \frac{Y^2}{k} \quad (6)$$

where Y is the charge on the shell and k is the harmonic spring constant.

Perfect lattice properties are calculated by allowing the unit cell to attain an energy minimum with zero forces on all the ions and cell parameters. Surfaces are similarly treated but here semi-infinite blocks are used where the ions nearest the surface are relaxed explicitly whilst more distant ions are held fixed. The MIDAS [24] code was used for the surface calculations reported here.

Bulk defect calculations are carried out using a two region strategy. Here ions in the inner region, surrounding the defect, are optimised explicitly

Table 1
Electron gas potential parameters

Species		Buckingham potential parameters		
		A (eV)	ρ (Å^{-1})	C (eV Å^{-6})
Mg^{2+}	O^{2-}	2134.39	0.2763	3.05
Mg^{2+}	O^{-}	4135.77	0.2255	0.49
O^{2-}	O^{2-}	676.90	0.3683	32.52
O^{-}	O^{-}	1396.51	0.2906	5.18
O^{2-}	O^{-}	889.64	0.3376	18.81
Li^{+}	O^{2-}	812.57	0.2725	0.97
Li^{+}	O^{-}	1583.43	0.2209	0.18

where $V(r) = Ae^{-r/\rho} - \frac{C}{r^6}$.
Buckingham potentials fitted from data of Colbourn et al. [35]; a cut-off of 12 Å was used for the short range interactions in all calculations

whilst the ions in the second (more distant) region respond as a continuum using the Mott–Littleton method [25]. Similar techniques are used for the surface with suitable modifications [26,27] to the Ewald method [28], used to sum the long range Coulombic interactions, as a consequence of the two dimensional nature of the surface. The two region methodology is implemented in the CASCADE [29] and CHAOS [30] codes for the bulk and surface respectively.

A large number of potentials have been derived for simulating MgO [16–18,31], most of which have been based on empirical fitting, a procedure which may give very accurate reproduction of perfect lattice properties. However, to model defects in the present system, potential parameters for Li_2O would have to be transferable to the host MgO lattice. Furthermore, electronic defects (i.e. oxygen holes) are to be considered. Thus, the present set of potentials was derived using the electron gas methods [32–34], which allows the development of a set of potential parameters which have all been derived in the same Madelung field, that of the host lattice. Consequently, the potentials are consistent with each other and problems associated with transferring potentials from one structure to another are avoided. Although this method does not generate potentials which reproduce the perfect lattice properties as well as those derived empirically, it has been demonstrated that potentials derived in this way return good defect energies in such materials [17,18].

Table 2
Shell model parameters, from Colbourn et al. [35]

Species	Shell charge Y	k (eV Å^{-2})
O^{2-}	−2.42	27.4623
O^{-}	−1.42	27.4623

where the free ion polarisability is given by $\alpha = \frac{Y^2}{k}$.

The parameters used are the electron gas potentials originally derived by Colbourn et al. [35] which were re-fitted to Buckingham functions for this work. These parameters are presented in Table 1. The shell model parameters for the lattice oxygen were empirically fitted by Colbourn et al. [35] to reproduce as well as possible the dielectric properties of MgO. The shell model spring constant and the core charge of O^- were assumed to be the same as O^{2-}, as used successfully by Colbourn et al. [35] (Table 2).

3. Results and discussion

3.1. Verification of potentials

In order to verify that the potentials are satisfactory, perfect crystal properties and defect formation energies have been calculated using these potentials, and have been compared to results for a number of empirically fitted potentials and quantum mechanical calculations [36,37]. The results for the perfect lattice of MgO are presented in Table 3 whilst defect energies are given in Table 4. These results clearly demonstrate the reliability of the potentials used in this study.

3.2. Surface structure and stability

Prior to discussing the defect chemistry and the nature of the active sites at the surface, we must first determine the structure of the non-defective surfaces of MgO. The dominant surface in MgO is the (1 0 0) face. However, morphological studies [9] show that the surface of MgO can consist

Table 3
Perfect lattice properties of MgO

Property	Electron gas potentials [a]	Empirical potentials [b]	Expt [c]
Lattice energy (eV)	−40.60	−39.48	−40.79
Lattice parameter (Å)	2.171	2.112	2.106
Elastic constants (10^{11} dyne cm^{-2})			
C_{11}	34.76	27.89	31.0
C_{12}	19.75	10.53	9.6
C_{44}	19.75	10.53	16.0
Dielectric constants			
static ϵ_0	9.91	9.42	9.86
high-frequency ϵ_∞	2.96	2.84	2.96

Calculations using the potentials to be used in this work are compared to other calculated and experimental values.
[a] As given in Table 1 and 2.
[b] Using the potentials of Catlow et al. [16]
[c] From the work of Peckham [53].

of terraces on the (1 0 0) surface which are of the order of ca. 100 Å across and can be considered as surfaces with high Miller indices of the general form (1 0 x). These low coordinate step sites have been suggested as possible sites for dopants [18] and also as possible active sites [9]. To select a suitable surface as a model for these steps we have determined the relaxed surface geometry and energy (given in Fig. 1) of the (1 0 x) series of surfaces with $x = 0, \ldots, 11$. As is usual, we present the surface energies (in Fig. 1) in terms of the misorientation angle θ where $\tan\theta = 1/x$ for a surface (1 0 x), which is a measure of the extent to which a surface deviates from the (1 0 0) surface towards the (1 1 0) surface. We find that for the (1 0 0) surface, the relaxation lowers the surface energy by a very small amount. Furthermore, the surface energy and surface rumpling (ca. 2%) are in excellent agreement with experimental measurements [38] and LEED data [39] respectively. For more stepped surfaces, the relaxation effects are much greater, this being reflected in the enhanced relaxation energy. However, as we might expect, as the Miller index of the surface increases, and the surface resembles more closely the (1 0 0) surface, we find that the energy of the surface approaches that of the (1 0 0) surface. The simulation results described above are in line with the results of Duffy et al. [19] on MgO and with the recent computational studies of the stepped (1 0 0) surface of NiO [40] which found a similar smooth variation of surface energy with misorientation angle. A small relaxation observed for the (1 0 0) surface was also found in high quality quantum mechanical calculations [41].

The (1 0 11) surface has an inter-step distance of 23.2 Å, which is of the order of four times the

Table 4
Formation energies for bulk defects in MgO

Defect	Calculated energy/eV	Other calculated values/eV	
		Atomistic simulations [a]	Quantum mechanical [b]
cation vacancy	25.30	24.40	26.38
anion vacancy	23.02	22.90	23.77
Schottky energy	7.46	7.55	8.28 (6.88 [c])
cation–anion vacancy pair	45.66	–	–
vacancy pair binding energy	−2.66	–	–
O^- trapped hole	15.40	–	–
Li^+ substitutional energy	16.18	16.27	17.90
$[Li]^O$ formation	30.83	–	–
$[Li]^O$ binding energy	−0.75	−0.99	–

The Li^+ substitutional energy is the energy required to remove a Mg^{2+} cation from a lattice site to infinity and replace it with a lithium. Similarly the formation energy of the $[Li]^O$ is the energy required to remove adjacent Mg^{2+} and O^{2-} ions and replace them with Li^+ and O^- ions.
[a] Simulation studies of Mackrodt and Stewart [17] and Foot and co-workers [54,55].
[b] Quantum mechanical studies of Grimes et al. [36].
[c] This value from De Vita et al. [37].

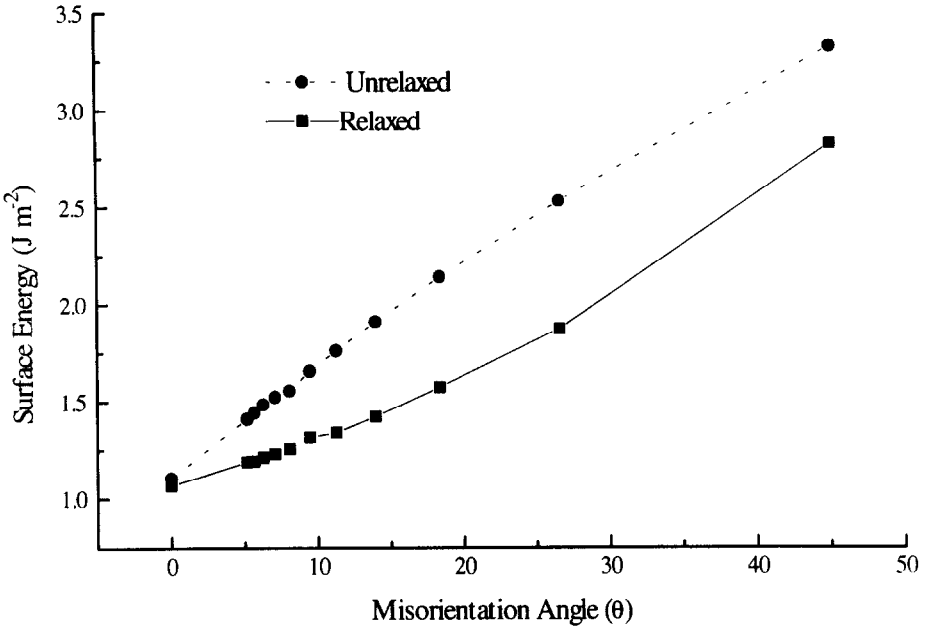

Fig. 1. The unrelaxed and relaxed surface energies for the series of surfaces (1 0 x) with $x=0, \ldots, 11$. The misorientation angle is defined as $\tan(\theta) = 1/x$, so that $\theta=0$ implies a (1 0 0) surface and $\theta=45°$ implies a (1 1 0) surface.

extent of any appreciable distortions produced in these calculations by defect formation. The energy of the surface is within 0.12 eV m^{-2} of that of the (1 0 0) surface and we therefore consider it to be a suitable model for independent step sites on the surface. We also note, that in typical crystals of MgO, terraces on the (1 0 0) surface are of the order of 100 Å in length [9,42,43] and thus we can expect experimentally that defects on steps act independently from similar defects at adjacent terraces. Thus, the (1 0 11) surface was selected as a model step surface.

The terraced nature of the surface of MgO suggests that active sites may be present at such low coordination sites. To investigate further the possible siting of active sites at low coordinate sites we shall consider the smallest terrace possible: a square dimer of MgO on the (1 0 0) surface (as shown in Fig. 2). We can consider this structure as the first step in the construction of a larger terrace by surface migration and rearrangement processes and also to be the lowest coordinated site at the surface. The relative stability of defects at this *protostep* will be considered particularly with reference to the (1 0 0) surface and the extended terraces described previously by the (1 0 11) surface.

3.3. Surface defects

Results are presented for defects which are thought to be involved in the partial oxidation reactions. These defects are considered in the bulk, on the (1 0 0) surface, at stepped surface sites and at protosteps. We will compare the stability of the defects at the different sites and will discuss the consequences of the results for the activity of the material.

Lithium trapped holes on the (1 0 0) surface

Experiment shows that holes are trapped by the presence of alkali metal ions in alkaline earth lattices [44]. Thus, the neutral lithium trapped hole defect centre is expected to be stable in Li/MgO. The binding energy of this defect is defined as the energy released when previously isolated lithium substitutional ions and localised oxygen hole defects are bought together at adjacent lattice sites:

$$Li_{Mg^{2+}(\infty)} + O_{O^{2-}(\infty)} \rightarrow [Li^{+}O^{-}] \qquad (7)$$

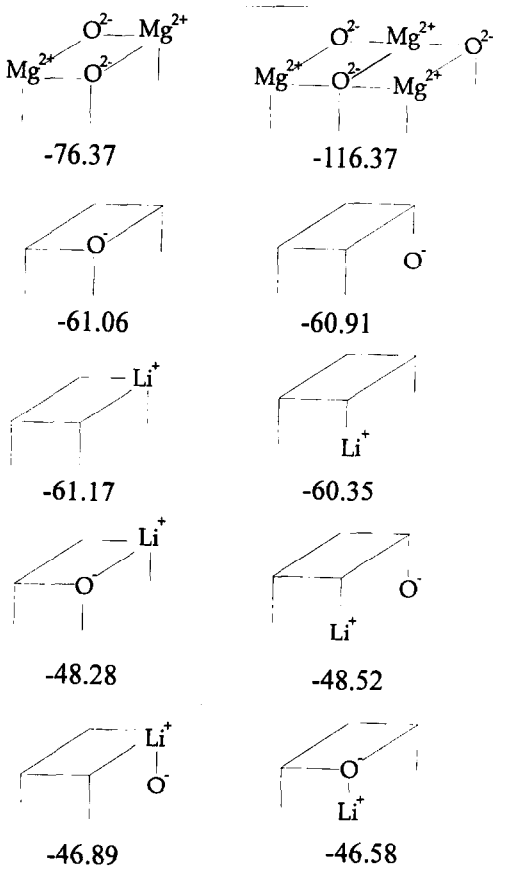

Fig. 2. The formation energies of various protostep structures on the (1 0 0) surface of MgO.

which gives a hole binding energy of;

$$E_{\text{bind}} = E([\text{Li}]^{\text{O}}) - E(\text{Li}^{+}_{\text{sub}}) - E(\text{O}^{-}_{\text{O}^{2-}}) \qquad (8)$$

Our calculations (Table 4) show that in the bulk, the $[\text{Li}]^{\text{O}}$ centre is bound, by 0.75 eV. Furthermore, we calculate a higher binding energy at the surface (1.1 eV) (see tables). We shall show later how $[\text{Li}]^{\text{O}}$ centres at low-coordinate sites are even more strongly bound.

The analysis described above relies upon a description of the hole defect as a localised species. In fact, it is well established that in the bulk of MgO, the hole is delocalised [20]. Thus, an additional energy term, that required to localise the hole on a single oxygen ion, must be included. This energy has been determined to be ≈ 0.6 eV [20] and consequently the binding energy of the hole to the Li ion is reduced to 0.15 eV. In the case of the surface, the hole localisation energy is probably slightly negative [20] and the binding energy is therefore unchanged. If, therefore, holes and Li^+ substitutional species are available on the surface, $[\text{Li}]^{\text{O}}$ centres will be expected to predominate. The next section examines therefore the relative energies of bulk and surface defects.

Surface stability and (1 0 0) surface segregation of defects

The formation energy of the Li^+ substitutional, the localised oxygen hole and the lithium trapped hole on the (1 0 0) surface of MgO are given in Table 5. The Li^+ substitutional ion has a surface segregation energy (the difference between the energy of the defect at the bulk and at the surface) of ≈ 0.2 eV. The $[\text{Li}]^{\text{O}}$ centre is much more strongly segregated with a surface segregation energy of ≈ 0.5 eV. We have also noted that it is more strongly bound at the surface. Therefore, we would expect these centres not only to be stable surface species but also to be present in much higher concentrations than the isolated defects in both the bulk and at the surface. The localised O^- is less stable at the surface although only by 0.1 eV. We have previously calculated [45] that there is a migration barrier for the $[\text{Li}]^{\text{O}}$ centre immediately below the surface layer, from which we would expect that migration of this defect from the surface into the bulk would be slow. The isolated defects on the other hand do not exhibit such a large barrier and therefore migration into the bulk would be quicker. However, as previously

Table 5
The formation energies and surface segregation energies of defects on the (1 0 0) surface of MgO and Li/MgO

Defect	Defect energy/eV	Surface segregation energy/eV [a]
cation vacancy	24.77	−0.53
anion vacancy	23.24	0.22
Schottky energy	7.14	−0.32
Li^+ substitutional	15.94	−0.24
O^- trapped hole	15.5	+0.1
$[\text{Li}]^{\text{O}}$ centre	30.36	−0.47
$[\text{Li}]^{\text{O}}$ binding	−1.1	–

[a] Surface segregation energy $= E_{\text{surface}} - E_{\text{bulk}}$. Negative values indicate that surface segregation is energetically favourable.

Table 6
Formation energies of defects at the (1 0 11) step site

Defect	Energy (eV)	Step segregation energy (eV)
cation vacancy	23.76	−0.01
anion vacancy	22.34	0.10
Li^+ substitutional	15.26	−0.68
O^- trapped hole	14.89	−0.61

The step segregation energy is defined as the difference between the defect energy at the (1 0 0) surface and at the step, with a negative value indicating that the defect at the step is energetically favoured.

noted, the $[Li]^O$ centre is likely to be the dominant surface defect species and is unlikely to dissociate to a significant extent; surface $[Li]^O$ centres are therefore expected to be stable.

Defects at step sites

We next explored the formation energies of the cation and anion vacancies at step sites, which, as is clear from the results reported in Table 6, are similar to those for the perfect (1 0 0) surface; the anion vacancy is in fact calculated to be less energetically favourable at the step. We note that the formation of vacancies at steps act essentially to lower the Miller index of the surface, a process which we have shown to increase the surface energy and we would therefore expect this process to be relatively unfavourable. From these results we might expect the formation of the cation, anion vacancy pair to be similarly unfavourable at the step. Calculations on such complex surface defects configurations are unfortunately beyond the capabilities of present simulation codes. However, our results do confirm that the smaller terraces are less stable as previously determined by the perfect surface calculations. Given therefore the high defect formation energy and the increase in surface energy, migration of ions away from terraces is likely to be slow.

The results for the O^- and Li^+ substitutional ion show a marked preference for the lower coordination step site. We would therefore expect any untrapped holes to be trapped at such sites. We would also expect from the results for the isolated defects that the $[Li]^O$ centre would also prefer step sites. Again, unfortunately the complexity of this defect precluded accurate simulation with the presently available code. However, the preference of the $[Li]^O$ centre for other low coordinate sites (protosteps) will be shown below.

Protosteps

Several relevant protosteps are shown in Fig. 2 together with their formation energies. The protostep formation energy is defined as the change in energy when the constituents of the protostep are bought from infinity and placed on the (1 0 0) surface. We shall consider first the formation of the non-defective protostep. We have already shown how the stability of a terraced surface increases and approaches that of the lowest energy surface, the (1 0 0) surface, as the length of the terrace increases. The equivalent process for a protostep is to compare the energy of different sized protosteps with the energy to add a complete 2-D layer of MgO onto an existing (1 0 0) surface (with respect to the equilibrium surface and the corresponding ions at infinity). The energy for the complete process is −40.2 eV per MgO. The energy to add an isolated protostep, 2MgO, is −38.2 eV. If we add a third MgO unit to form a 3MgO protostep, there is a further stabilisation leading to an energy of −38.8 eV per MgO. We can see therefore that, given conditions suitable for migration of surface species, small protosteps will aggregate to form extended surfaces, a process evident for clean MgO surfaces which rearrange on annealing to maximise the (1 0 0) surface area [42].

We shall now consider the protostep as a site for defects involved in partial oxidation catalysis. We have calculated energies for the reactions summarised by the Eqs. 9–12 (depicted in Scheme 1), which show that the protostep is indeed a more favourable site not only for the $[Li]^O$ centre (Eqs. 9, 10) but also for its components, the small polaron (Eq. 11) and the lithium substitutional ion (Eq. 12).

These effects are primarily a result of the reduced electrostatic field at such sites. The results are consistent with those found for the Li substitutional and oxygen hole defects at the (1 0 11)

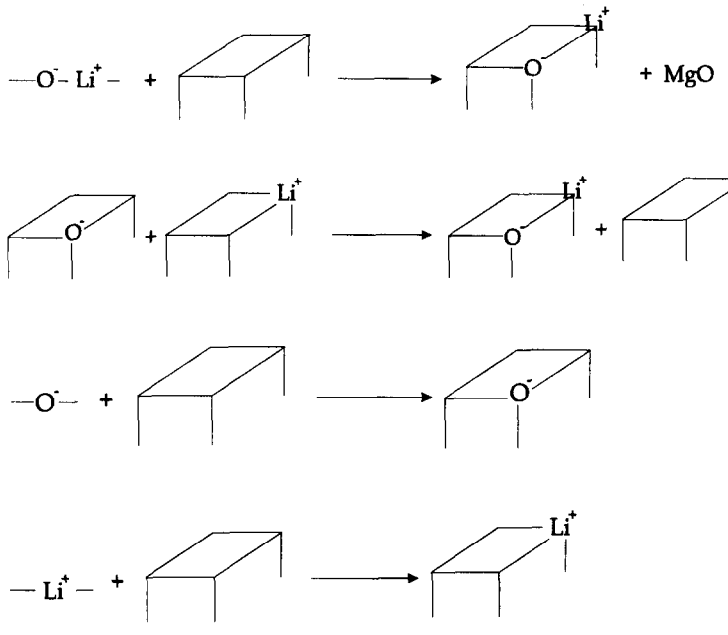

Scheme 1.

step. We also note that the binding energy of the $[Li]^O$ centre is increased at the protostep (Eq. 10) compared to the (1 0 0) surface, being respectively 2.4 eV and 1.1 eV. The result for the $[Li]^O$ centre (Eq. 9) also supports our general conclusions that defects will segregate to low coordination sites, e.g., steps.

Unlike the case of the defects at the top of protosteps, the bottom of the protostep does not appear to be particularly favourable for the trapping of either a hole or of the lithium substitutional (Eqs. 13–14, Scheme 2) over that of a perfect (1 0 0) surface. However, we find that the $[Li]^O$ centre is more stable at this site than at the top of the protostep (Eq. 15, Scheme 2). We note that Hargreaves et al. [9] suggested that dislocations may act as traps for $[Li]^O$ centres when they emerge at the surface. The stability of the $[Li]^O$ centre at the bottom of steps can be considered as having a similar immobilising effect.

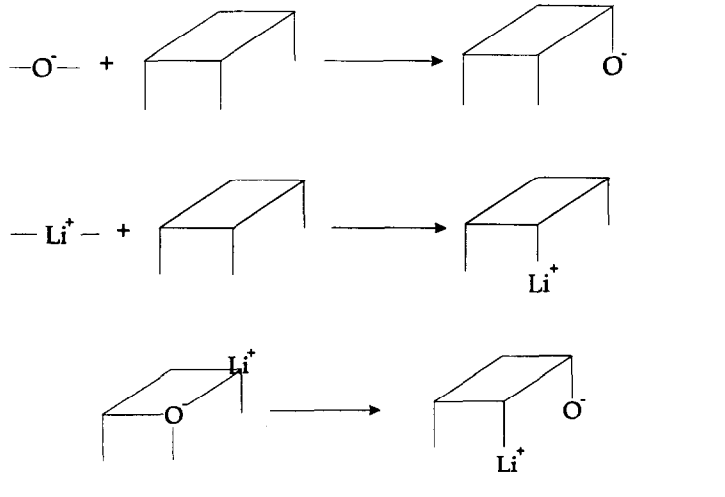

Scheme 2.

Table 7
Binding energy and oxygen hole formation energies at different sites

Oxygen site	Coordination number of the oxygen	$[Li]^O$ binding energy (eV)	Hole formation energy $O^{2-} \rightarrow O^-$	
			no Li	adjacent to Li
bulk	6	−0.75	6.00 [a]	5.85
(1 0 0) surface	5	−1.10	6.70	5.62
PS top Li top	3	−2.42	6.51	4.09
PS top Li bottom	3	−1.54	6.51	4.97
PS bottom Li top	6	−1.18	6.60	5.48
PS bottom Li bottom	6	−3.63	6.60	3.03

The binding energy is as given in Eq. 8. PS is a protostep and the associated Li is given as the adjacent lattice site either at the top or bottom of this protostep (as illustrated in Fig. 2).
[a] Assumes the isolated hole in the bulk is delocalised [20].

Finally we considered the two situations in which the $[Li]^O$ centre was orientated perpendicular to the (1 0 0) surface: in the first instance the Li^+ is at the top of the protostep and in the second at the bottom (see Fig. 2). In both cases these configurations were less stable than when the $[Li]^O$ centre is at either the top or the bottom of the step. We do not therefore expect that these configurations will be stable, since hole hopping will allow re-orientation to other configurations.

Ionisation of O^{2-}

We are now in a position to determine the ionisation energy of O^{2-} ions located at a variety of sites in MgO and Li/MgO. The negative of the energy, i.e. the electron affinity of the O^- hole state, is a direct measure of the power of the centre for abstraction of electrons from gas phase reactants e.g. hydrocarbons. The ionisation energy is calculated as the difference in defect energy between O^{2-} and O^- to which we add the second electron affinity of oxygen, i.e. the change in the intra-atomic energy of the oxygen ion on losing an electron. This electronic energy term has previously been calculated at 8.8 eV [17]. The use of this value for MgO is supported by additional Hartree–Fock calculations [46].

Our calculated energies are reported in Table 7. We note the substantial reduction in the ionisation energy at sites adjacent to Li. We compare our results with those of Abarenkov and Frenkel [47] who determined the ionisation energy of an O^{2-} at an edge site in MgO to be 7 eV, using ab initio quantum mechanical techniques. Despite this good agreement, we should emphasise the approximate nature of these calculations; and it is the differences in energies which should receive attention rather than their absolute values.

4. Comments on the reaction mechanism

We shall now place the above results in the context of proposed reaction mechanisms of partial oxidation of methane and the selectivity and activity of the MgO based catalysts. We shall also comment on the relative activity and selectivity of different possible active sites on the basis of their calculated stability.

4.1. The formation of oxygen holes and the effect of lithium

We have seen how lithium binds strongly to an oxygen hole, a result which also indicates that the presence of lithium will lower the energy required to form these holes. This effect is clearly shown in Table 7, where we give the energy to form a hole at several sites, in the presence and absence of lithium. For all the sites considered, the presence of Li^+ lowers the energy to form the localised hole. Of particular note is the significant decrease in the energy at the bottom of protosteps.

Another important consideration is the presence or otherwise of localised hole species in undoped MgO; experimentally some methane activation is noted in the pure material. As mentioned previously [20], it has been demonstrated that oxygen holes delocalise in the bulk, the delocalisation state being stabilised by ~0.6 eV, whilst at the flat (1 0 0) surface the energies of the localised and delocalised states are rather similar. When this additional energy term is considered we see that the delocalised bulk hole is more stable than that at the (1 0 0) surface (by 0.7 eV) and at the (1 0 11) step (by 0.4 eV). Essentially, the ability of the hole to delocalise in the bulk means that the hole is more stable in the bulk rather than at the (1 0 0) surface. But, the energetic preference of the hole for the bulk is decreased if low coordinate sites are available. Nevertheless, even then, it seems that the hole is more stable in the bulk than on the surface. Conversely, if Li^+ ions (or presumably other monovalent impurities) are present, the hole becomes more stable at the low coordinate sites to which the impurity ions will segregate. Thus we conclude that localised holes are unlikely to be present at the (1 0 0) surface in pure MgO, although there could be some stabilisation by intrinsic defects. For example we calculate that the V^0 centre (i.e. 2 holes trapped at a cation vacancy) is bound by 3.2 eV. But we may expect such a defect to be less active for methane activation than a trapped hole, as it contains two active species distributed over 3 lattice sites. Furthermore the geometry of this site is more akin to ethane than methane; and we note that Burch and Tsang demonstrated that pure MgO is more active for ethane than methane.

4.2. *Defect stability as an indicator of activity*

Experimentally, the $[Li]^O$ centre is considered to be the main active site for hydrogen abstraction from methane. However, it has also been shown that although this site activates both methane and ethane, other active sites are present at which ethane is more readily dehydrogenated [48]. It should also be remembered that the C–H bond strength in methane is higher than in ethane (435 kJ mol^{-1} and 410 kJ mol^{-1} respectively), suggesting that if the $[Li]^O$ centre were equally active for both methane and ethane then much higher yields of ethene than are achieved would be expected. Thus, other active sites must be present for the dehydrogenation of ethane and other surface catalysed reactions. We shall now discuss the relative activity of the $[Li]^O$ centre and untrapped holes at both planar and step sites and attempt to relate this to possible reaction pathways.

We can consider that the more *stable* a catalytically active centre, the *less active* it will be. Conversely an unstable species is likely to be highly active and may indeed be simply reactive rather than catalytically active. We can apply these principles to the active sites here by considering the relative activity of these defects at the various surface topographic features.

Consider first the activity of the $[Li]^O$ centre. We have shown that the stability of this centre is highest at the low coordinate sites such as steps. Thus if the morphology of the catalyst results in the formation of many of such sites, we predict that the $[Li]^O$ centre will segregate to these sites. The concentration of the most active hydrogen abstraction centres (from methane) will be correspondingly reduced and we may expect a decrease in the conversion of methane. The total number of $[Li]^O$ centres will, however, remain constant since we find that this centre is still bound at the low coordination sites. Furthermore, the increased stability of these step $[Li]^O$ centres may result in them being less active for methane activation whilst maintaining their ethane activity, owing to the lower C–H bond strength in the latter molecule. This suggests that a morphology which promoted the siting of $[Li]^O$ centres at low coordinate sites will lead to an overall decrease in the activity of the catalyst but may increase selectivity to ethene production. However, following our assumption that a more stable active site will be less active, we also suggest that there will be an increase in the activation energy of the reaction involved.

4.3. Morphological effects and activity

The recent work by Hargreaves et al. [9] has concluded that the primary active site for ethane and ethene formation is located at the (1 0 0) surface; but they also propose from their morphology studies that the *bottom* of steps may also be active for hydrocarbon conversion. From our results, we can conclude that $[Li]^{O}$ centres will segregate to step sites. Thus any morphological change which promotes the formation of low coordinate sites will have a significant effect on catalytic activity.

We have also demonstrated here that localised holes are unlikely to be present at the surface of pure MgO. The activity (albeit limited) of pure MgO and the effect of morphology on this activity as demonstrated by Hargreaves et al. [9] therefore suggests that active sites other than oxygen holes are also active in this reaction. We note that F centres have been postulated as active sites [49–51] and furthermore recent quantum mechanical calculations have shown that the formation energy of F centres is decreased at low coordinate surface sites [52]. Our findings are consistent with the view that other defects e.g. V centres, are also active for methane coupling and that it is feasible that these sites are present at low coordinate sites.

5. Conclusions

The calculations reported in this paper have substantial implications both for our general understanding of the surface chemistry of magnesium oxide and related materials and for the specific questions relating to the catalytic activity of the material. We have found that relaxed stepped surfaces are of low energy – a result that is fully consistent with the experimental data of Hargreaves et al. [9] and others showing the common occurrence of terraced surfaces in this material. Next, we have further clarified the role of the Li dopant: Li^{+} not only increases the overall concentration of holes, but also promotes their segregation to surface sites where they may act as catalytic centres for partial oxidation reactions; the catalytic activity of pure MgO is probably attributed to more complex intrinsic surface defects. Thirdly, out calculations have emphasised the crucial role of surface morphology in determining catalytic activity. Low coordinate surface sites are traps for the $[Li]^{O}$ centres. The resulting trapping will modify considerably the catalytic activity, and may influence strongly the selectivity for specific partial oxidation reactions.

Acknowledgements

The EPSRC are acknowledged for general financial support and the provision of funds to DWL. RWG would like to thank the Gas Research Institute for financial support. Professor Sir John M. Thomas and Dr. Alexander. L. Schluger are thanked for useful discussions.

References

[1] T. Ito, J.-X. Wang, C.H. Lin and J.H. Lunsford, J. Am. Chem. Soc., 107 (1985) 5062.
[2] T. Ito and J.H. Lunsford, Nature, 314 (1985) 721.
[3] D.J. Driscoll and J.H. Lunsford, J. Phys. Chem., 87 (1983) 301.
[4] D.J. Driscoll, W. Martir, J.-X. Wang and J.H. Lunsford, J. Am. Chem. Soc., 107 (1985) 58.
[5] D.J. Driscoll and J.H. Lunsford, J. Phys. Chem., 89 (1985) 4415.
[6] D.J. Driscoll, W. Martir, J.-X. Wang and J.H. Lunsford, in M. Che and G.C. Bond (Eds.), Adsorption and Catalysis on Oxide Surfaces, Elsevier, Amsterdam, 1986, p. 403.
[7] J.H. Lunsford, C.-H. Lin, J.-X. Wang and K.D. Campbell, in M.J. Treacy, J.M. Thomas and J.M. White (Eds.), Microstructure and Properties of Catalysts, Vol. 3, Materials Research Society, Pittsburgh, 1988, p. 305.
[8] G.J. Hutchings, J.R. Woodhouse and M.S. Scurrell, J. Chem. Soc., Faraday Trans. I, 85 (1989) 2507.
[9] J.S.J. Hargreaves, G.J. Hutchings, R.W. Joyner and C.J. Kiely, J. Catal., 135 (1992) 576.
[10] G.J. Hutchings, M.S. Scurrell and J.R. Woodhouse, Chem. Soc. Rev., 18 (1989) 251.
[11] S.P. Mehandru, A.B. Anderson and J.F. Brazdil, J. Am. Chem. Soc., 110 (1988) 1715.
[12] E.A. Colbourn and W.C. Mackrodt, Surf. Sci., 117 (1982) 571.
[13] E.A. Colbourn and W.C. Mackrodt, Solid State Ionics, 8 (1983) 221.

[14] E.A. Colbourn, J. Kendrick and W.C. Mackrodt, Surf. Sci., 126 (1983) 550.
[15] J.H. Harding, Rep. Prog. Phys., 53 (1990) 1043.
[16] C.R.A. Catlow, I.D. Faux and M.J. Norgett, J. Phys. C, 9 (1976) 419.
[17] W.C. Mackrodt and R.F. Stewart, J. Phys. C, 12 (1979) 5015.
[18] E.A. Colbourn and W.C. Mackrodt, J. Mat. Sci., 17 (1982) 3021.
[19] D.M. Duffy, J.P. Hoare and P.W. Tasker, J. Phys. C, 17 (1984) L195.
[20] A.L. Shluger, R.W. Grimes, C.R.A. Catlow and N. Itoh, J. Phys.-Cond. Matter, 3 (1991) 8027.
[21] P.W. Tasker and D.M. Duffy, Surf. Sci., 137 (1984) 91.
[22] C.R.A. Catlow and W.C. Mackrodt (Eds.), Computer Simulation of Solids, Vol. 166, Spinger-Verlag, Berlin, 1982.
[23] B.G. Dick and A.W. Overhauser, Phys. Rev., 112 (1958) 90.
[24] P.W. Tasker, AERE-R9130, AERE Harwell, 1978.
[25] N.F. Mott and M.J. Littleton, Trans. Faraday Soc., 34 (1938) 485.
[26] D.E. Parry, Surf. Sci., 49 (1975) 433.
[27] D.E. Parry, Surf. Sci., 54 (1976) 195.
[28] R.P. Ewald, Ann. Physik, 64 (1921) 253.
[29] M. Leslie, AERE-R7650, Daresbury Laboratory Report, 1982.
[30] D.M. Duffy and P. Tasker., R11059, Harwell Report, 1983.
[31] G.V. Lewis and C.R.A. Catlow, J. Phys Chem., 18 (1985) 1149.
[32] P.T. Wedepohl, Proc. Phys. Soc., 92 (1967) 79.
[33] R.G. Gordon and Y.S. Kim, J. Chem. Phys., 56 (1972) 3122.
[34] J.H. Harding and A.H. Harding, R10425, AERE Harwell, 1982.
[35] E.A. Colbourn, J. Kendrick and W.C. Mackrodt, ICI Report, IC00852/2.
[36] R.W. Grimes, C.R.A. Catlow, A.L. Schluger, R. Baetzold and R. Pandey, Ceram. Trans., 24 (1991) 269.
[37] A. De Vita, M.J. Gillan, J.S. Lin, M.C. Payne, I. Stich and L.J. Clarke, Phys. Rev. Lett., 68 (1992) 3319.
[38] W.C. Mackrodt and R.F. Stewart, J. Phys. C, 10 (1977) 1431.
[39] M.R. Welton-Cook and W. Berndt, J. Phys. C, 15 (1982) 5691.
[40] M. Yan, S.P. Chen, T.E. Mitchell, D.H. Gay, S. Vyasand R.W. Grimes, Phil. Magn., 72 (1995) 121.
[41] S. Pugh and M.J. Gillan, Surf. Sci., 320 (1994) 331.
[42] M. Gajdardziskajosifovska, P.A. Crozier, M.R. McCartney and J.M. Cowley, Surf. Sci., 284 (1993) 186.
[43] P.A. Crozier, M. Gajdardziskajosifovska and J.M. Cowley, Microsc. Res. Tech., 20 (1992) 426.
[44] Y. Chen and M.M. Abraham, J. Phys. Chem. Solids, 51 (1990) 747.
[45] D.W. Lewis and C.R.A. Catlow, Top. Catal., 1 (1994) 111.
[46] R.W. Grimes Report TP1308, AEA Harwell, 1988.
[47] I.A. Abarenkov and T.Y. Frenkel, J. Phys.-Cond. Matter, 3 (1991) 3471.
[48] J.H. Lunsford, P.G. Hinson, M.P. Rosynek, C.L. Shi, M.T. Xu and X.M. Yang, J. Catal., 147 (1994) 301.
[49] M.C. Wu, C.M. Truong, K. Coulter and D.W. Goodman, J. Am. Chem. Soc., 114 (1992) 7565.
[50] M.C. Wu, C.M. Truong and D.W. Goodman, Phys. Rev. B, 46 (1992) 12688.
[51] M.C. Wu, C.M. Truong, K. Coulter and D.W. Goodman, J. Catal., 140 (1993) 344.
[52] L.N. Kantorovich, J.M. Holender and M.J. Gillan, Surf. Sci., (1995) in press.
[53] G. Peckham, Proc. Phys. Soc., 90 (1967) 657.
[54] J. Foot MSc. Thesis, University of Keele, 1988.
[55] J.D. Foot, E.A. Colbourn and C.R.A. Catlow, J. Phys. Chem. Solids, 49 (1988) 1225.